PL-TR-94-2141

REVISED NOISE MODEL OF THE MSX SPIRIT III INTERFEROMETER

Alexander S. Zachor

Atmospheric Radiation Consultants, Inc.
59 High Street
Acton, MA 01720

20 May 1994

Scientific Report No. 1

PHILLIPS LABORATORY
Directorate of Geophysics
AIR FORCE MATERIEL COMMAND
HANSCOM AFB, MA 01731-3010

"This technical report has been reviewed and is approved for publication"

JAMES J. GIBSON
Contract Manager

WILLIAM A.M. BLUMBERG
Branch Chief

ROGER A. VAN TASSEL
Division Director

This report has been reviewed by the ESC Public Affairs Office (PA) and is releasable to the National Technical Information Service (NTIS).

Qualified requestors may obtain additional copies from the Defense Technical Information Center. All others should apply to the National Technical Information Service.

If your address has changed, or if you wish to be removed from the mailing list, or if the addressee is no longer employed by your organization, please notify PL/TSI, Hanscom AFB, MA 01731-3010. This will assist us in maintaining a current mailing list.

Do not return copies of this report unless contractual obligations or notices on a specific document requires that it be returned.

REPORT DOCUMENTATION PAGE

Form Approved
OMB No. 0704-0188

1. AGENCY USE ONLY (Leave blank)	2. REPORT DATE	3. REPORT TYPE AND DATES COVERED
	20 May 1994	Scientific No. 1

4. TITLE AND SUBTITLE
Revised Noise Model of the MSX SPIRIT III Interferometer

5. FUNDING NUMBERS
PE 63215C
PR S321
TA GD
WU AC
Contract F19628-93-C-0044

6. AUTHOR(S)
Alexander S. Zachor

7. PERFORMING ORGANIZATION NAME(S) AND ADDRESS(ES)
Atmospheric Radiation Consultants, Inc.
59 High Street
Acton, MA 01720

8. PERFORMING ORGANIZATION REPORT NUMBER

9. SPONSORING/MONITORING AGENCY NAME(S) AND ADDRESS(ES)
Phillips Laboratory
29 Randolph Road
Hanscom AFB, MA 01731-3010
Contract Manager: J. Gibson/GPOS

10. SPONSORING/MONITORING AGENCY REPORT NUMBER
PL-TR-94-2141

11. SUPPLEMENTARY NOTES

12a. DISTRIBUTION/AVAILABILITY STATEMENT
Approved for public release; distribution unlimited

12b. DISTRIBUTION CODE

13. ABSTRACT *(Maximum 200 words)*

A preliminary model for predicting the performance of the MSX SPIRIT III interferometer has been implemented as a computer code module that provides estimates of expected total noise and saturation levels. This report gives the theoretical development of the model and includes usage instructions for the code. A later version of the code will be used in the automated analysis of SPIRIT III interferometer data at the Phillips Laboratory Data Analysis Center. The model has provided predictions of system performance in planned MSX experiments for remote sensing of atmospheric trace constituents.

14. SUBJECT TERMS			15. NUMBER OF PAGES
MSX	noise model	remote detection	34
SPIRIT III	limb radiance	stratosphere	16. PRICE CODE
interferometer	trace species	mesosphere	

17. SECURITY CLASSIFICATION OF REPORT	18. SECURITY CLASSIFICATION OF THIS PAGE	19. SECURITY CLASSIFICATION OF ABSTRACT	20. LIMITATION OF ABSTRACT
UNCLASSIFIED	UNCLASSIFIED	UNCLASSIFIED	SAR

CONTENTS

PREFACE

The work described herein was sponsored by the Air Force Materiel Command under Contract No. F19628-93-C-0044. The author wishes to thank the following persons for valuable guidance, data or helpful discussions: Robert O'Neil and Harold Gardiner of the Phillips Laboratory/GPO, and Clair Wyatt and Tom Woolston of the Space Dynamics Laboratory at Utah State University. Thanks are due also to the coauthors of the paper reproduced in the Appendix for technical guidance and help in preparing the manuscript of the paper.

INTRODUCTION

Described in this report is a preliminary model for predicting the performance of the MSX SPIRIT III interferometer. The model provides estimates of the expected noise and saturation levels of the instrument in measuring spectral radiances of the Earth and its limb. (The Appendix and its references describe the the MSX program and SPIRIT III interferometer).

This "noise model" of the SPIRIT III interferometer is implemented as a computer code module named IFR_NOIS, which will be part of the Earthlimb automated analysis capability for processing MSX data at the Phillips Laboratory Data Analysis Center (PL DAC). The module's primary subroutine is IFR_NOISE. In the DAC automated spectral analysis, this subroutine (as well as many others involved in screening, indexing and cataloging the interferometer data) will be "driven" by the routine IFR_SPC_DRIVER. The current version of IFR_NOISE is Revision 1c, dated 28 April 1994.

The primary purpose of the present report is to provide a user's guide for subroutine IFR_NOISE and to present some performance predictions based on this noise model. The first three sections define the purpose of the routine, and provide related background material and detailed usage instructions. These sections constitute the user's guide.

The section entitled *Theoretical Basis* fully documents the equations and conventions upon which the noise calculations are based. It assumes familiarity with the interferometer system design, which is described in Ref. 1 and in works cited in Section 1.2 of Ref. 1. A discussion of the qualitative effects of the several noise sources treated in the present noise model will be found in Ref. 2. (Also given in Ref. 2 are interferometer performance predictions based on an earlier, very crude noise model; these are superseded by predictions based on the model described herein.)

The section entitled *Interferometer Parameters* lists the instrument specifications used in the current noise model, such as the fields of view, collector area, etc., that determine its capabilities. These data are represented as constants in the subroutine. (Filter spectral transmissions, which are supplied to the routine via common storage, are not listed.) Some of the "specifications," such as the interferometer's wavelength-dependent modulation index, are based on engineering data and recent tests at SDL. The listed specifications are believed to be up-to-date as of early July, 1993. The subroutine is structured such that the interferometer parameter values are easily changed.

The remaining sections give the channel Noise Equivalent Spectral Radiances (NESRs) and other predictions of the noise model. The Appendix is a preprint of a paper that used the present noise model to predict the performance of the SPIRIT III interferometer in planned MSX experiments for remote sensing of atmospheric trace constituents.

It is emphasized that this report describes a preliminary version (Rev. 1c) of the interferometer noise model. The final version of the model (module IFR_NOIS, Rev. 2) will be delivered to PL in May or June 1994. Revision 1c is essentially a predictive model based on given "efficiencies" for the system's optical components and detectors. Revision 2 will use preflight calibration data in place of most of these efficiencies; it will be more of an empirical model. The present report supersedes the ARC technical report describing Revision 0 of the noise model.[3]

PURPOSE

Subroutine IFR_NOISE can be used to estimate the total system noise for the MSX SPIRIT III interferometer. The returned total noise includes the effects of

a) preamp-Johnson noise (system dark noise, which determines the NESR),
b) photon noise, and
c) digitization noise from A/D conversion.

The spectral-domain, total-noise estimate depends on the length and apodization of the interferogram (i.e., on the effective spectral resolution) and on the scene spectral radiance observed by the interferometer. The scene contributes photon noise; it also determines the automatic gain setting which, in turn, determines the A/D noise level.

The subroutine can also be used to compute just the Noise Equivalent Spectral Radiance (NESR) or to return just a scale factor SF by which the NESR should be multiplied to obtain the total noise.

BACKGROUND

The automated analysis of MSX SPIRIT III interferometer data, as charted in Fig. 3-36 of the Earthlimb Automated Analysis Plan (EAAP)[4], produces a template spectrum and noise spectrum for each measured (CONVERT) spectrum that is analyzed. Summary product spectra will show the measured spectral radiance and total noise spectral radiance in the same plot (usually the larger of the two values at each wavelength). Subroutine IFR_NOISE, and the section of the calling procedure that assigns the actual arguments for the subroutine, constitute the procedure labeled "ESTIMATE SYSTEM TOTAL NOISE SPECTRUM" in the EAAP flowchart.

The use of different operational modes in the subroutine offers flexibility in how noise estimates are obtained. For example, the calling procedure can compute NESRs for the six channels once-and-for-all, and thereafter use the routine only to obtain scale factors SF. It can elect to use only NESRs obtained from engineering test data or a DCATT calibration sequence and scale these by SF to obtain the total noise.

The arguments supplied by the calling procedure include interferogram length/apodization parameters and a "source" spectrum. The source spectrum (which is required only when total noise or SF is to be computed) will usually be one obtained from measured data via the Canonical CONVERT program; the length/apodization parameters would be those used in the CONVERT processing. For modeling expected performance or when the S/N in the observed spectrum is expected to be low, the calling procedure may want to supply a template spectrum as the source spectrum. The calling procedure can either supply a gain setting or direct the routine to predict the automatic gain level.

USAGE

Subroutine IFR_NOISE requires spectral transmittance data for the six interferometer filters; this data is assumed to exist in the two dimensional array *filt_trans* in common block GET_IFR_DAT. The subroutine is invoked by the Fortran statement

```
CALL IFR_NOISE( MODE, ICHAN, LASER, IATYP, ALPHA, LEN_APO,
   RESLN, GAINACT, GAIN2, GAIN1, SPECTRUM, LEN_SPC, WAVN1, DELW,
   TOT_NOIS, SF, BPR, ICLIP, IERR, SATBPR, EFFM )
```

where:

MODE determines the operational mode:
- = -1 if the NESR is to be returned.
- = 0 if the scale factor SF ({total noise}/NESR) is to be returned.
- = 1 if both total noise (NESR times SF) and SF are to be returned.

The NESR is returned in array SPECTRUM. Other parameters (see below) determine its spectral range and the spacing of the spectrum samples.

ICHAN = the channel number for the NESR, SF, or total noise.

LASER determines which laser reference is in operation:
- = 0 if the primary (HeNe) laser is in use
- = 1 if the solid state laser is in use

IATYP selects the apodization function to be represented in finding the spectral resolution that the NESR or total noise will correspond to:
- = 0 for no apodization
- = 1 for triangular apodization
- = 2 for Kaiser-Bessel (K-B) apodization

ALPHA = value of parameter α in the K-B window function (if IATYP = 2)

LEN_APO = number of samples, after two-sided truncation/apodization, to be used in finding the spectral resolution.

RESLN = the computed spectral resolution (returned in cm^{-1})

GAINACT, if not zero, is a supplied gain for channel ICHAN.
If the supplied GAINACT is zero, the routine sets the gain internally to the computed value GAIN2. (When MODE = -1, the supplied GAINACT is not used and GAIN2 is not computed/returned.)

GAIN2 = the theoretical automatic gain as determined from the supplied spectral radiance SPECTRUM, and assuming the band photon radiance is increasing (high-gain side of hysteresis loop); GAIN2 is computed and returned if MODE is not -1 (whether or not GAINACT is zero).

GAIN1 has the same definition as GAIN2, except decreasing band photon radiance is assumed (low-gain side of hysteresis loop).

SPECTRUM is a supplied or returned array of spectral radiances:
If MODE is not -1, it is a supplied radiance spectrum over channel ICHAN representing what the interferometer "sees," i.e., a spectrum from Canonical CONVERT or a predicted (template) spectrum. Parameters LEN_SPC, WAVN1 and DELW define the spectral range and spacing. Values in a supplied SPECTRUM are expected in the units W/cm^2 sr cm^{-1}.
If MODE is -1, it is the returned NESR spectrum in W/cm^2 sr cm^{-1}.

LEN_SPC = the length of array SPECTRUM; LEN_SPC, WAVN1 and DELW are supplied (input) parameters.

WAVN1 = the wavenumber (cm^{-1}) represented by the first element of SPECTRUM.

DELW = the wavenumber spacing (cm^{-1}) of spectral radiances in SPECTRUM.

TOT_NOIS = the returned total noise spectrum in W/cm^2 sr cm^{-1} if MODE = 1. LEN_SPC, WAVN1 and DELW define the spectral range and spacing. When MODE is -1 or 0, array TOT_NOIS is used as workspace; i.e., its contents prior to the subroutine call are not preserved.

SF (if MODE is 0 or 1) is the returned scale factor. Multiplying a NESR spectrum by SF converts it to a total noise spectrum.

BPR = the Band Photon Radiance (ph/s cm^2 sr) corresponding to SPECTRUM if MODE is 0 or 1 (see *Theoretical Basis* Section).

ICLIP is returned, if MODE is 0 or 1, to indicate whether the interferometer channel is predicted to be clipped:
= 0 if the fringes are not clipped for the supplied SPECTRUM
= 1 if the fringes are clipped

IERR is a returned error indicator:
= 0 if no error
= 1 if the spectral filter for channel ICHAN is not completely within the spectral range defined by the supplied values of LEN_SPC, WAVN1 and DELW. (Filter bands are defined by arrays *lam1s* and *lam2s*; this data is assumed to exist in common block FILT_CUTOFFS.)

SATBPR = the BPR that causes interferogram central fringe clipping; returned only if MODE is 0 or 1 (see BPR and *Theoretical Basis* Section).

EFFM = the effective modulation index, defined as the computed central fringe ac interferogram value divided by the computed dc level; returned only if MODE is 0 or 1.

Note that the calling procedure, which is normally part of the automated SPIRIT III spectral analysis, will have knowledge of how individual interferograms were processed by Canonical CONVERT. In other words, the calling procedure is supplied values for ICHAN, LASER, IATYP, ALPHA and LEN_APO by Standard CONVERT and/or Canonical CONVERT and the DCE Experiment Script. The calling procedure, in turn, supplies these values to subroutine IFR_NOISE.

The largest values to be expected for LEN_APO are roughly 8220 and 4110 samples, respectively, for even and odd ICHAN values. These correspond to the maximum scan time of 4.3 s, with 0.14 s lost to turnaround. The total retardation change X over the two-sided scan equals drive velocity times effective scan time, approximately 0.25 OPD cm/s times 4.16 s, or 1.04 cm (OPD is optical path difference, or retardation). The above estimates for LEN_APO equal $X/\Delta x$, where Δx is one of the two HeNe sampling intervals given by Eq. (1) in the *Theoretical Basis* section. Use of these values for LEN_APO implies that the long interferograms have been zero-filled to the transform array sizes 16384 and 8192, respectively.

An anticipated CONVERT processing option is to slightly truncate the long interferograms to 8192 and 4096 samples, in which case these would be the appropriate values to supply for LEN_APO. The corresponding unapodized resolution is approximately 0.96 cm^{-1}; this is the value of RESLN that would be returned when IATYP = 0.

THEORETICAL BASIS

This section defines the noise model for the SPIRIT III interferometer in terms of equations and conventions implemented in subroutine IFR_NOISE. The subroutine's dummy arguments appear in capital letters and are as defined in the above *Usage* section. (Identical notation is used in this section, in the above *Usage* section and in the Fortran source code for the dummy arguments, but not for other quantities.) The order in which

quantities are calculated in the subroutine and in this description of the noise model is roughly the same.

The input parameter LASER is used to specify which laser is being used in the interferometer reference channel to sample the interferogram. If LASER is zero, the primary (HeNe) laser is in use, and the laser wavelength λ_L is assigned the value 0.632985 μm. If LASER is not zero, the solid state laser is being used, and λ_L is set to 0.6700 μm.

The input parameter ICHAN is the interferometer channel number for the current subroutine calculations. The sampling interval Δx is twice λ_L for the even-numbered channels and four times λ_L for the odd-numbered channels; i.e., the even-numbered channels are located at relatively short wavelengths (high wavenumbers) and must be sampled at a higher rate than the odd-numbered channels. The subroutine obtains Δx in cm as

$$\Delta x = (\mathrm{MOD}(\mathrm{ICHAN},2) + 1) * 2.0 * \lambda_L * 10^{-04}. \quad (1)$$

The calculated Δx and other quantities are used to estimate the spectral resolution and the parameter k1, defined below.

The length, in samples, of the two-sided interferogram after truncation, if any (including any truncation effected by an apodization that the calling procedure wants to represent), is specified by the input parameter LEN_APO. The corresponding length in cm is Δx times LEN_APO. The reciprocal of this length is the resolved spectral interval Δν, if the interferogram was not apodized. The subroutine calculates a factor *rf* (*resfac* in the source code) that accounts for the effect on resolution of any apodization that the calling procedure wants to be represented in the noise calculation. Thus, the resolved spectral interval in cm^{-1} is obtained as

$$\Delta\nu = rf / (\Delta x * \mathrm{LEN\_APO}) \quad (2)$$

The subroutine allows the specification of three apodization "types" via the input parameter IATYP: Values of 0, 1 and 2 correspond to "no apodization," triangular apodization and Kaiser-Bessel (K-B) apodization, respectively; the length of the apodization window is LEN_APO. When IATYP is 2, the additional input parameter ALPHA specifies the value of α in the K-B window function, where the window function and α are as defined by F. J. Harris.[5] The factor *rf* evaluates to 1.0 if IATYP = 0, to 2.0 if IATYP = 1, and to ALPHA if IATYP = 2. The computed Δν is the distance to the first zero in the instrument line shape (which is the Fourier cosine transform of the apodization window function). The computed Δν is exact when IATYP is 0 or 1, and is approximate when IATYP is 2. The subroutine returns Δν as RESLN.

The parameter k1 calculated by the routine converts quantities normally specified in per root-Hz units (such as NEP) to per wavenumber (cm^{-1}) units. As shown by Wyatt[6], this parameter can be cast in the form

$$k1 = (v_0 / \Delta v)^{1/2}, \tag{3}$$

where v_0 is the drive velocity of the interferometer in OPD cm/s. The calculated k1 has the units cm $Hz^{1/2}$. The calculated NESR and total noise includes k1 as a factor; i.e., these noise spectra vary as $\Delta v^{-1/2}$.

The calculation of the interferometer noise requires the spectral transmission of the filter in channel ICHAN. This spectrum is supplied to the routine via an array in common. Hereafter, the filter spectral transmission for channel ICHAN will be denoted $t_F(i)$, where i is a spectrum index. For channel 5, $t_F(i)$ includes the effect of IFOV reduction by a mask.

In preparation for the calculation of spectrum noise, the routine obtains the mean-square preamp noise voltage v_p, the mean-square thermal noise voltage v_t and the resultant rms dark noise voltage v_{dn}:

$$v_p = (2\pi R_L C_T E_n)^2 F^3 / 3, \tag{4}$$

$$v_t = 4kTR_L F, \tag{5}$$

$$v_{dn} = (v_p + v_t)^{1/2}, \tag{6}$$

where

R_L is the feedback resistance of the Trans-Impedance Amplifier (TIA) preamp,
C_T is the TIA input capacitance,
E_n is the TIA input noise voltage,
T is the temperature of the preamp and detectors, and
F is the information noise bandwidth of channel ICHAN.

These, of course, are voltages in the time (interferogram) domain.

The noise-equivalent spectral radiance (NESR) depends on the above dark noise voltage v_{dn}, various constant efficiency factors and efficiencies dependent on channel and/or wavelength, like beamsplitter net efficiency, modulation index, $t_F(i)$ and detector quantum efficiency. The routine has a loop over wavenumber that searches and interpolates in pre-defined data arrays to establish values for most of the spectrally varying quantities. In the same loop the routine integrates over an optionally supplied scene radiance spectrum to obtain the "Band Photon Radiance" (BPR). The BPR determines the photon noise contribution to the total noise, as well as the maximum of the ac component of the interferogram. The latter is used to estimate the automatic gain setting and the

resultant A/D noise contribution. The spectral integration and the calculation of BPR and gain is not performed when the calling procedure specifies that only the NESR is to be returned.

The calling procedure specifies a wavenumber mesh and spectral range over which the NESR or total noise will be calculated. This is also the mesh on which the scene spectral radiance is supplied if the total noise or scale factor SF is to be calculated. The routine finds the detector quantum efficiency q(i) (assumed to be the same for all detectors/channels) and the filter spectral transmission $t_F(i)$ interpolated onto this mesh. The vectors q(i) and $t_F(i)$ will now denote interpolated values rather than values in a data statement or common array; these are indexed by wavenumber, whereas the original data values are defined on a wavelength grid.

Let $\lambda(i)$ denote the wavelength in μm corresponding to index i, i.e., to wavenumber $\nu(i)$ in the user-defined mesh. The voltage responsivity r(i) of the detector at this wavelength is calculated as

$$r(i) = r_{20}*(\lambda(i)/20)*q(i)/q_{20}, \tag{7}$$

where r_{20} and q_{20} are the detector responsivity and quantum efficiency, respectively, at wavelength 20 μm. A corresponding NEP is obtained as

$$NEP(i) = v_{dn} / (F^{1/2}*r(i)). \tag{8}$$

Finally, the NESR(i) is calculated as

$$NESR(i) = k1*NEP(i) / (A_c*\Omega*t_e*t_F(i)). \tag{9}$$

where

A_c is the collecting area of the entrance aperture,
Ω is the solid angle IFOV for channel ICHAN,
$t_e = t_t*t_{bs}*m$
t_t is the telescope reflectivity for channel ICHAN,
t_{bs} is the FTS cube (beamsplitter, etc.) net efficiency, and
m is the modulation index.

Both t_{bs} and m are functions of wavelength in the current version of the noise model. The NESR values returned by the subroutine have the units Watts/cm^2 sr cm^{-1}.

An alternative form for Eq. (7) is

$$r(i) = r_{20}*R_d(i), \tag{10}$$

where

$$R_d(i) = (\lambda(i)/20)*q(i)/q_{20} \qquad (11)$$

is the detector relative response. Similarly, Eq. (8) can be written as

$$NEP(i) = NEP(\lambda_p) / R_d(i), \qquad (12)$$

where $NEP(\lambda_p) = v_{dn}/(F^{1/2}*r(\lambda_p))$ is the NEP at peak spectral response, i.e., the response at $\lambda = \lambda_p \approx 20$ μm. Substituting Eq. (12) into (9) and writing $R_d(i)*t_F(i) = R_S(i)$, where $R_S(i)$ is the "system spectral response function," results in the following alternative expression for the NESR:

$$NESR(i) = k1*NEP(\lambda_p) / (A_c*\Omega*t_e*R_S(i)). \qquad (13)$$

USU provided a file of the detector relative response R_d. This file and Eq.(11) were used to obtain a set of quantum efficiencies q for subroutine IFR_NOISE.

As indicated earlier, a user-supplied radiance spectrum is required only when the total noise and/or scale factor SF is to be returned. The supplied spectrum will be denoted N_ν. It represents spectral radiance in per cm^{-1} units versus wavenumber ν. The corresponding interferogram voltage vs. retardation x at the TIA is

$$vs(x) = R_L e\, t_t A_c \Omega \int_{Chan} \frac{N_\nu q_\nu t_{F\nu} t_{bs}}{hc\nu} \frac{[1 + m\cos(2\pi\nu x)]}{2}\, d\nu, \qquad (14)$$

where e is the elementary charge and hc is Planck's constant times the speed of light. In this equation, q_ν and $t_{F\nu}$ represent the quantities q(i) and $t_F(i)$, defined earlier. The integral is over the wavenumber range of channel ICHAN.

The Band Photon Radiance (BPR) is defined as the effective dc photon radiance (ph/s cm^2 sr) at the entrance aperture:

$$BPR = \int_{Chan} \frac{N_\nu q_\nu t_{F\nu} t_{bs}}{hc\nu}\, d\nu. \qquad (15a)$$

Analogous to the dc and ac components of the interferogram (see Eq. 14), we define BPR to be a dc term and BPRm to be the corresponding ac term:

$$BPRm = \int_{Chan} m \frac{N_\nu q_\nu t_{F\nu} t_{bs}}{hc\nu} \, d\nu. \tag{15b}$$

Hereafter, vs_{ac} will denote the ac voltage at the central fringe (at x = 0) and vs_{dc} will denote the dc voltage. Using Eqs.(14) and (15) these voltages can be written

$$vs_{dc} = R_L * e * (t_t/2) * A_c * \Omega * BPR, \tag{16a}$$

$$vs_{ac} = R_L * e * (t_t/2) * A_c * \Omega * BPRm. \tag{16b}$$

The dc photon spectrum (photons/s cm^{-1}) impinging on the detector is

$$\phi_{p\nu} = (t_t/2) * A_c * \Omega * N_\nu * t_{F\nu} * t_{bs} / hc\nu. \tag{17}$$

Using Eqs.(15a) and (17) we can write (16a) in the form

$$vs_{dc} = R_L e \int_{Chan} \phi_{p\nu} q_\nu \, d\nu. \tag{18}$$

The rms of the photon noise voltage throughout the interferogram is given by

$$v_{pn} = R_L e \left[2F \int_{Chan} \phi_{p\nu} q_\nu \, d\nu \right]^{1/2}, \tag{19}$$

which, from Eq.(18), can be written

$$v_{pn} = (R_L * e * vs_{dc} * 2F)^{1/2}. \tag{20}$$

The routine obtains BPR and BPRm according to Eqs.(15), vs_{ac} and vs_{dc} from Eqs.(16), and then calculates v_{pn} from Eq.(20). Yet to be determined is the A/D noise level in the interferogram.

The number of counts C out of the 12-bit A/D converter corresponding to a given interferogram ac maximum voltage vs_{ac} is

$$C = [(2^{12} - 2) * (vs_{ac} + 5 v.) / 10 v.) + 1] * G, \quad (21)$$

where G is the gain setting. Thus, the number of counts produced at unit gain by the system when vs_{ac} is -5, 0 and 5 volts is 1, 2048 and 4095 (= $2^{12} - 1$), respectively. In automatic-gain mode, the gain is decreased by a factor of two each time an *increasing* number of counts at the interferogram maximum exceeds a certain C value. Similarly, a factor-of-two gain increase occurs when the maximum counts are *decreasing* and falls below a particular C value. At unit gain the two voltages that effect automatic gain changes are 3.75 v. and 3.75/4 = 0.9375 v. For an arbitrary gain setting G we conclude (using these two voltage levels and Eq. 21) that gain changes occur when $|C-2048|$ equals 2^{b1} or 2^{b2}, where b1 = 8.58426 and b2 = 10.58426. This is the same as saying automatic gain changes correspond to an interferogram ac maximum (absolute value) which is equivalent to approximately 8.584 or 10.584 bits at the current gain setting.

Subroutine IFR_NOISE uses Eq.(21), the above b1 and b2 values, and the known maximum gains for the six channels to determine the automatic gain setting corresponding to vs_{ac}. The routine actually returns two values, GAIN2 and GAIN1, corresponding to an increasing and decreasing signal, respectively. As described below, it also determines whether the interferogram central fringes are predicted to be clipped.

The calling procedure can supply a value for input parameter GAINACT, which if non-zero is used by the routine as the actual gain setting (which has been reported, presumably, by CONVERT). If the supplied value is zero, the routine uses the calculated GAIN2 as the current gain setting. The maximum gains G_{max} for the six interferometer channels were supplied by USU, and are defined in a DATA statement in the subroutine.

The A/D noise voltage at the TIA, which will be denoted v_{ad}, is defined as that corresponding to an uncertainty of 1/2 in the count level C. By using Eq.(21) to equate a change ΔC of 1/2 to a change $\Delta vs_{ac} = v_{ad}$ and solving for v_{ad}, we obtain

$$v_{ad} \cong (10 v. / 2^{12}) / (2*G), \quad (22)$$

where G is the current gain setting. This equation is used by the routine to obtain the A/D noise voltage.

The routine obtains the total noise voltage at the TIA as the root-sum-square of the three noise components:

$$v_{tn} = (v_{dn}^2 + v_{pn}^2 + v_{ad}^2)^{1/2}. \quad (23)$$

Finally, it obtains the returned scale factor SF as the ratio of total noise to dark noise:

$$SF = v_{tn} / v_{dn}. \quad (24)$$

Although SF is obtained from voltages in the time domain, it is also the ratio of total spectrum noise to the NESR. Thus, the total noise, which is returned as the array TOT_NOIS, is calculated from

$$\text{TOT\_NOIS}(i) = \text{SF} * \text{NESR}(i). \tag{25}$$

The gain can have one of seven levels ranging between G_{max} and $G_{min} = G_{max}/2^6$. Clipping of the interferogram occurs when the gain has its minimum value while |C-2048| exceeds 10^{11}. The routine finds the corresponding BPR level above which the interferogram is clipped and returns it as SATBPR. The routine also returns a value for ICLIP; it is 1 if BPR ≥ SATBPR and 0 otherwise.

The routine also calculates and returns an "effective" modulation efficiency EFFM, defined as the ratio of ac to dc voltage at the interferogram center, i.e., EFFM = vs_{ac}/vs_{dc} = BPRm / BPR.

Many interferometer parameters, such as A_c and the wavelength-dependent beamsplitter efficiency t_{bs}, are assigned values through PARAMETER and DATA statements in the subroutine code. This is also true of the full-scale A/D input voltage v_{fs}, the number of A/D bits N_{ad}, the gain-switching bit levels, etc., even though their assigned (actual SPIRIT III) values have been used in the above text and equations to simplify the discussion; e.g., v_{fs} = 10 v. and N_{ad} = 12.

The wavelength-dependent modulation index m is computed from a fifth-order polynomial evaluated by a short function routine included in module IFR_NOIS. Subroutine IFR_NOISE includes a data statement defining the six coefficients needed by the function. Each reference to the function routine supplies these coefficients and defines the wavelength for which the modulation index is to be computed.

INTERFEROMETER PARAMETERS

This section lists the constants in subroutine IFR_NOISE that define the interferometer noise. Table 1 shows only those constants needed by the routine in calculating the NESR corresponding to a particular spectral resolution. The modulation index m at wavelength W is computed by the routine as

$$\begin{aligned} m = &(c1 + W (c2 + W (c3 + W (c4 + W (c5 + W\, c6))))) / 100, \text{ with} \\ &c1 = 2.734896, \quad c2 = -0.5068297, \quad c3 = 0.9076166, \quad c4 = -0.07671653 \\ &c5 = .002503216, \quad c6 = -0.00002928215. \end{aligned} \tag{26}$$

Table 1. Parameters of the SPIRIT III interferometer noise model that affect NESR

Large detector IFOV (sr)	1.37E-05
Small detector IFOV (sr)	5.14E-06
Collector area (cm^2)	393.0
Drive velocity (OPD cm/s)	0.250

PARAMETER/CHANNEL	1	2	3	4	5	6
Telescope reflectance...	0.932	0.911	0.932	0.922	0.919	0.922
Information noise bandwidth (Hz).....	300	1200	600	1200	600	1200

Filter spectral transmittances: per files supplied on floppy disk by USU/SDL as of 6/21/93

TIA feedback resistance (ohms)	9.0E+07
TIA input capacitance (farads)	4.0E-11
TIA input noise (volts)	1.0E-07
TIA operating temperature (deg K)	10

Detector responsivity at 20 μm (V/W).....1.26E+09

Detector quantum efficiency Q vs. wavelength λ in μm:

λ	Q	λ	Q	λ	Q	λ	Q
2.0	.4230	2.5	.3800	3.0	.2800	3.5	.2800
4.0	.3700	4.5	.4000	5.0	.3800	5.5	.3100
6.0	.3500	6.5	.3420	7.0	.3320	7.5	.3520
8.0	.3970	8.5	.3860	9.0	.4470	9.5	.4450
10.0	.5080	10.5	.5340	11.0	.5770	11.5	.6350
12.0	.6170	12.5	.6180	13.0	.6830	13.5	.7050
14.0	.7400	14.5	.6780	15.0	.7900	15.5	.7370
16.0	.9250	16.5	1.0300	17.0	.9330	17.5	.9060
18.0	.8460	18.5	.8120	19.0	.7900	19.5	.7810
20.0	.7930	20.5	.7740	21.0	.7960	21.5	.8660
22.0	.8650	22.5	.8650	23.0	.8650	23.5	.9000
24.0	.8640	24.5	.7770	25.0	.6600	25.5	.5640
26.0	.4880	26.5	.3670	27.0	.2660	27.5	.1540
28.0	.0830	28.5	.0370	29.0	.0146	29.5	.0108
30.0	.0070	30.5	.0000				

Beamsplitter net efficiency tbs vs. wavelength λ in μm:

λ	tbs	λ	tbs	λ	tbs	λ	tbs
2.0	.0250	2.5	.0265	3.0	.0280	3.5	.0420
4.0	.0600	4.5	.0650	5.0	.0700	5.5	.0730
6.0	.0760	6.5	.0840	7.0	.0960	7.5	.1020
8.0	.1160	8.5	.1100	9.0	.1050	9.5	.1160
10.0	.1270	10.5	.1160	11.0	.1010	11.5	.1000
12.0	.0980	12.5	.1200	13.0	.1400	13.5	.1500
14.0	.1600	14.5	.1600	15.0	.1600	15.5	.1600
16.0	.1670	16.5	.1610	17.0	.1560	17.5	.1560
18.0	.1560	18.5	.1470	19.0	.1370	19.5	.1310
20.0	.1240	20.5	.1180	21.0	.1120	21.5	.1000
22.0	.0880	22.5	.0790	23.0	.0700	23.5	.0650
24.0	.0600	24.5	.0500	25.0	.0400	25.5	.0310
26.0	.0210	26.5	.0160	27.0	.0100	27.5	.0080
28.0	.0060	28.5	.0030	29.0	.0010	29.5	.0010
30.0	.0001	30.5	.0000				

For the listed value of drive velocity, the internally computed frequency conversion factor k1 (see Eq. 3 in the *Theoretical Basis* section) evaluates to 0.509 cm $Hz^{1/2}$ for the case of an unapodized, long interferogram. The spectrally resolved interval for this case (see Eq. 2) is approximately 0.96 cm^{-1} if the interferogram is not apodized.

Table 2 lists the additional constants needed to predict the gain level and/or total noise for a given input radiance spectrum.

Table 2. Additional parameters of the SPIRIT III interferometer noise model

```
A/D full-scale input volts..................................... 10
Number of A/D converter bits................................... 12
AC bits for gain reduction.....................................10.58426
AC bits for gain increase.....................................8.58426
Maximum number of gain changes allowed.......................... 6
Factor by which gain is changed................................ 2.0
```

PARAMETER/CHANNEL	1	2	3	4	5	6
Maximum gain.....	357.3	64.0	140.8	64.0	140.8	64.0

CHANNEL NESRs

A simple driver program was written to test subroutine IFR_NOISE for MODE = -1 and obtain its prediction of the six channel NESRs. The resultant NESRs, corresponding to a long, unapodized interferogram ($\Delta\nu$ = 0.96 cm^{-1}) are shown in Figure 1. For

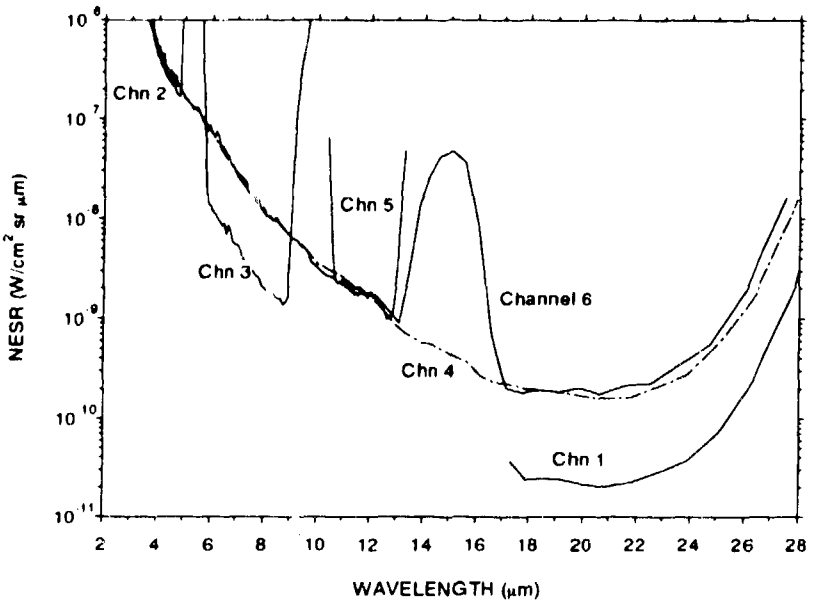

Figure 1. NESRs predicted for the SPIRIT III interferometer by the noise model code. The NESRs correspond to a spectral resolution of 0.96 cm^{-1}, unapodized.

comparison, the NESRs measured by SDL during a cold test in 1993 are shown in Figure 2. It is seen that the noise model does reasonably well in reproducing the spectral shapes of the measured NESRs, but does not accurately predict the actual NESR levels for all channels. The model consistently underestimates the NESR and predicts substantially lower NESRs than are measured for channels 2, 3 and 4.

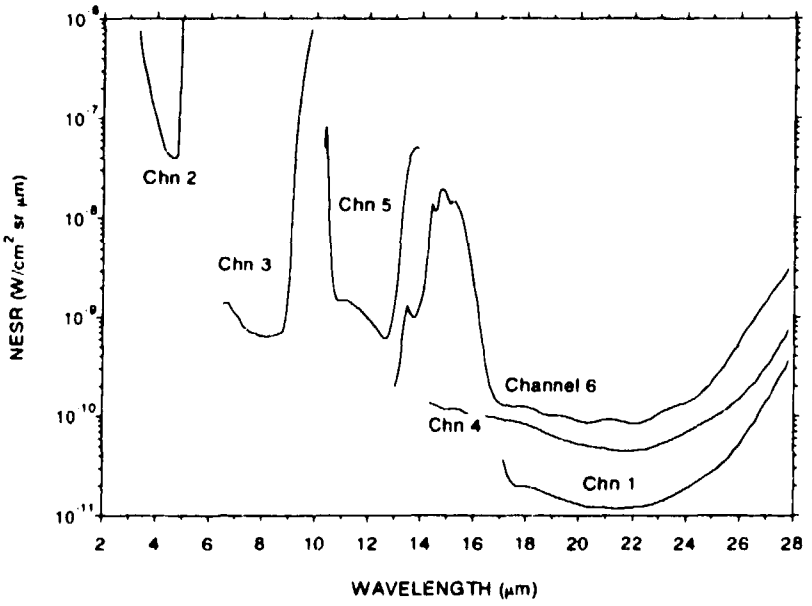

Figure 2. NESRs measured by SDL (after extrapolation to spectral resolution 0.96 cm^{-1} and removal of the A/D noise component).

These discrepancies led to the decision to develop another revision of the noise model. As stated earlier, the forthcoming Rev. 2 will be more of an empirical model, which will depend on measured rather than predicted NESRs. It will still be necessary in the Rev. 2 model to use estimated efficiencies for some optical components in order to predict the A/D and photon noise contributions to the total noise spectrum. However, it is anticipated that the revised noise model will provide much better accuracy in predicting total noise levels than the current Rev. 1c model.

The current interferometer noise model was developed both as an element of the MSX automated data processing and as a tool for estimating the performance to be expected in planned MSX experiments. The performance predictions described in the following section and in the Appendix are based on a temporary modification of the Rev. 1c model: Predicted NESRs for the six channels are each scaled by a constant so as to be in approximate agreement with the measured NESRs shown in Figure 2. The scaled NESRs are then combined with the model's prediction of A/D and photon noise to obtain the total noise spectrum. The Rev. 1c model is assumed to correctly predict gain settings and the occurrence of clipped interferograms.

OTHER MODEL PREDICTIONS

Another driver code for subroutine GET_NOISE was written to obtain estimates of the tangent height at which the interferogram becomes clipped, and the one at which the maximum S/N in the spectrum is approximately 10. These two H_T values, obtained for each channel, define the useful tangent height ranges of the SPIRIT III interferometer. The results are shown in Table 3. The limb radiance spectra required in these computations were generated by the MODTRAN code[7] for tangent heights H_T below 50 km, and by the SHARC code[8] for tangent heights above 50 km.

Table 3. Useful tangent height ranges for the six interferometer channels*

Chan	Wavelength range(μm)	H_T(km) for CLIP	H_T(km) for S/N_{max}=10
1	17-28	55	120
2	2.6-4.9	(NO CLIP)	70
3	5.8-8.9	30	90
4(OPEN)	4-29	60	160
5	10.4-13.2	8	90
6(PREW)	3-29	45	130

* Preliminary estimates

APPENDIX

Reproduced here is the camera-ready manuscript of the paper "Mid-Course Space Experiment (MSX): Capabilities of the LWIR interferometer for remote sensing of trace constituents in the stratosphere and mesosphere." The paper was presented at the Atmospheric Propagation and Remote Sensing III conference, part of SPIE's Optical Engineering/Aerospace Sensing symposium held on 4-8 April 1994 at Orlando, FL. The paper will appear in Proc. SPIE, vol. 2222 (1994).

The work reported in the paper is based on the described noise model except that measured NESRs were used to scale those predicted by the model, as noted in the section *Channel NESRs*.

Mid-Course Space Experiment (MSX): Capabilities of the LWIR interferometer for remote sensing of trace constituents in the stratosphere and mesosphere

Alexander S. Zachor
Atmospheric Radiation Consultants, Inc.,
Acton, Massachusetts 01720

William O. Gallery
Atmospheric and Environmental Research, Inc.,
Cambridge, Massachusetts 02139

Robert R. O'Neil, James Gibson and Harold A. B. Gardiner
U.S. Air Force Phillips Laboratory,
Hanscom AFB, Massachusetts 01731-3010

A. T. Stair, Jr.
Visidyne, Inc., Burlington, Massachusetts 01830

John D. Mill
Environmental Research Institute of Michigan,
Arlington, Virginia 22209

ABSTRACT

The planned Mid-Course Space Experiment (MSX) observations will include two experiments for remote detection of atmospheric trace constituents above 10 km altitude, based on measurements of limb spectral radiance by the cryogenic infrared interferometer and the ultraviolet and visible spectrographic imagers. Species to be monitored include: NO and CO_2 in the thermosphere, O_3 and H_2O in the mesosphere and stratosphere, HNO_3, CFC-11, CFC-12, N_2O and CH_4 in the stratosphere, and CO in the upper troposphere and lower stratosphere. Quantification of the altitude profiles of these species will give insight into processes affecting their global distributions and the atmosphere's response to anthropogenic perturbations, and contribute to further understanding of global change. The timing of the measurements is particularly advantageous since they will likely be the only regular limb observations of trace constituents during the operational lifetime of the MSX satellite. The SPIRIT III interferometer has a maximum spectral resolution of 1 cm^{-1} in six spectrally isolated channels whose vertical fields of view are between 4 and 13 km in line-of-sight tangent altitude. The six channels will provide spectra over wavelengths in the 2.6-28 μm range for tangent heights up to 180 km. The capabilities of the interferometer for the planned remote-sensing experiments, based on predicted instrument noise and saturation levels, are described in this paper .

1. INTRODUCTION

The Mid-Course Space Experiment (MSX) is a program funded and managed by the Ballistic Missile Defense Organization.[1] The comprehensive MSX mission and suite of instruments aboard the MSX satellite are described by Mill, et. al.[2,3] Planned MSX experiments[3,4] will gather spectroscopic and radiometric data on terrestrial, earthlimb and celestial scenes in support of ballistic missile defense objectives as well as for scientific pursuits in atmospheric remote sensing and astronomy.

The Fourier transform spectrometer and the LWIR radiometer (together called SPIRIT III) collect data through a shared 393 cm^2 aperture. A solid hydrogen cryogen with estimated 18-month lifetime cools both sensors, their foreoptics and the telescope baffle. An additional suite of instruments (called UVISI) includes five ultraviolet and visible spectrographic imagers. Experiments to define the earthlimb background against which midcourse surveillance systems will operate use the radiometer as the primary sensor and UVISI as a supporting system to provide diagnostic information on atmospheric composition and

temperature. They will measure radiance levels and fine-scale structure associated with aurora, airglow, mesospheric and noctilucent clouds, joule-heated atmospheres and stratospheric warmings, over a wide range of viewing conditions. The interferometer will lend additional diagnostic support by providing spectrally resolved data over the broad radiometer bands, although at much coarser spatial resolution than the radiometer.

Two planned MSX experiments depend on the capabilities of the SPIRIT III interferometer to remotely measure concentrations of trace species throughout the stratosphere and above, up to approximately 180 km. Since the species are observed in emission, their concentrations can be obtained for a wide range of geographic locations for both day and night conditions. Interferometer measurement programs based on solar occultation (like ATMOS[5]) are more limited in their global coverage and provide data only for daytime conditions. The cryogenic sensor technology represented by the SPIRIT III interferometer has been demonstrated by the similar CIRRIS 1A interferometer system[6] aboard Space Shuttle Discovery during the eight-day STS-39 mission.

In the following two sections we describe the interferometer's basic observational capability (its spectral ranges, spectral and spatial resolutions, and gain levels), and its performance (expected noise and saturation levels). Section 4 discusses the two remote sensing experiments and some features of the automated data reduction and cataloging procedures that pertain to all experiments using the interferometer. In Section 5 we give an estimate of the basic sensing capabilities of the instrument by listing the altitude ranges over which the following species can be detected: NO, NO_2, N_2O, HNO_3, CH_4, CO, CFC-11, CFC-12, O_3, aerosols, H_2O and CO_2.

The MSX system will be launched in November 1994 and will supply important data during a critical gap of six or more years between UARS[7] and the first EOS environmental satellite (POEM-ENVISAT[8]), expected to be launched after the turn of the century. The CLAES and ISAMS sensors on UARS have ceased operation, while the currently operating HALOE system performs occultation measurements limited to sunrise and sunset, ±75 degrees latitude, and cannot measure CFC's. The MLS sensor on UARS can measure only O_3, ClO and H_2O_2. In particular, the MSX interferometer, during its operational period, will be the only system capable of measuring vertical profiles of the critically important species N_2O, HNO_3, CO, CFC-11, and CFC-12 on a global scale. The data base of calibrated MSX measurements and results of their analysis will be available to the scientific community.

2. INTERFEROMETER DESCRIPTION

The MSX SPIRIT III interferometer has six arsenic-doped silicon blocked impurity band (Si:As/BIB) detectors with transimpedance amplifiers (TIAs) operating at approximately 11 degrees K. Figure 1, an object-space projection of the interferometer's focal plane, indicates the sizes and offsets of the six instantaneous fields of view (IFOVs). Distances read from the right-hand and upper scales are in a plane perpendicular to the optic axis at the line-of-sight tangent altitude (LOSTA), and are calculated for LOSTA = 60 km, a representative value for the remote sensing experiments. Optical filters over detectors 1, 2, 3, 5 and 6 limit their range of spectral response. The unfiltered channel 4 uses the full range of its detector, approximately 3 to 28 μm. The "prewhitened" filter in channel 6 passes nearly the same broad range of wavelengths but has a notch that attenuates over the region of the 15-μm CO_2 band. For limb observations the notch typically effects a slight reduction in photon noise and allows operation at higher gain, which reduces A/D noise. It lowers by approximately 10 km the LOSTA at which channel 6 is saturated compared to channel 4.

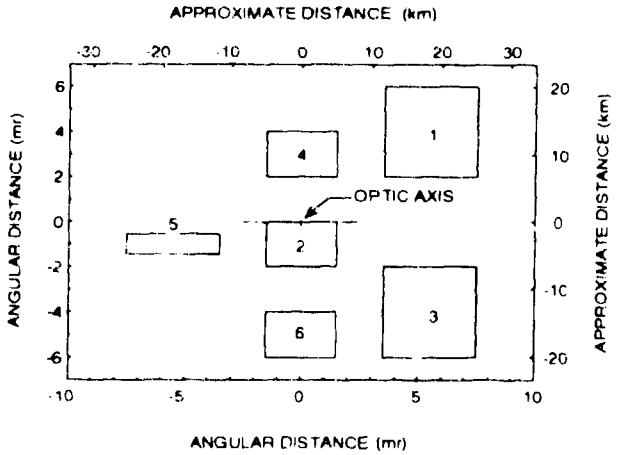

Figure. 1. The interferometer focal plane projected into object space. Distances on the right-hand and bottom scales are for a line-of-sight tangent altitude of 60 km.

The spectral coverage of each detector-channel, its vertical IFOV size and usable range in LOSTA are listed in Table 1. Near the bottom of the usable LOSTA range the instrument will be close to saturation (and provide maximum signal to noise), while at the top the S/N at the wavelength of maximum limb spectral radiance will be

approximately 10. These tangent height limits are based on predictions of the spectrally resolved earthlimb radiance profile and current estimates of the instrument's performance, and will likely be refined when preflight testing and calibration of the interferometer are completed. Useful data at LOSTAs above the ranges in Table 1 can be obtained by coadding interferograms, which is an option available in most MSX experiments.

Table 1. Characteristics of the six interferometer channels

Channel	Spectral range (μm)	Vertical resolution (mr)	Vertical resolution (km)	Approximate LOSTA range (km)*
5	10.5-13	1.17	4.0	8-90
2	2.6-4.9	1.85	6.3	0 (or nadir) to 70
3	5.8-8.9	3.7	12.5	30-90
1	17-28	3.7	12.5	55-120
4 (Open)	3-28	1.85	6.3	60-160
6 (Prewhitened)	3-26	1.85	6.3	45-130

* Preliminary estimates

Sensing of stratospheric trace constituents will utilize the capabilities of channels 5, 2 and 3, which are currently estimated to saturate at tangent altitudes of 8, 0 and 30 km, respectively. Channel 5 will observe the emissions of chlorofluorocarbons, nitric acid and other species. Channels 4 and 6, with saturation altitudes of 60 and 45 km, respectively, are used in one of the two remote sensing experiments, as described in Section 4. Channel 2 will not saturate even when pointed BTH (Below-The-Horizon) except possibly when the BTH scene includes specularly reflected sunlight. Its 2.6-4.9 μm spectral range provides support to SPIRIT III radiometer experiments that will measure Above-ATH (Above-The-Horizon) and BTH fine-scale spatial structure in the 4.3 μm CO_2 region[9], while allowing observation of the spectrum of sun-lit aerosols and remote sensing of some trace species not observable in the other interferometer channels at low LOSTAs. Channel 3 provides a capability to measure H_2O, CH_4 and NO_2 concentrations throughout the middle stratosphere and above.

Effects of nonlinearities associated with the high-performance Si:As/TIA combination are mitigated by recording and processing double-sided rather than single-sided interferograms. The interferograms have programmable lengths equivalent to unapodized resolutions of roughly 1, 2 and 10 cm^{-1} in wavenumber. The times required to record them are 4.3, 2.2 and 0.43 s, respectively. The resolutions of the device after minimal apodization to suppress sidelobes are approximately 2, 4 and 20 cm^{-1}. Experiments that monitor atmospheric trace constituents will produce spectra in the highest resolution mode.

The interferometer (IFR) system has a 12-bit A/D converter and seven gain levels which differ by multiples of two. Hence, it provides an effective range of 18 bits ($\approx 2.6 \times 10^5$) in the digitized signal. Users may program the gain level or opt to use automatic gain ranging. The auto-gain ranging logic is described in the following section. Additional information on the interferometer system are given in the SPIRIT III Sensor User's Guide.[10]

3. INSTRUMENT PERFORMANCE

The primary instrument effects in the IFR data are preamp-Johnson (dark) noise, digitization or "A/D" noise, and photon noise. These have corresponding components in the spectrum obtained by Fourier analysis of the interferogram. The noise-equivalent spectral radiance (NESR) is the dark spectrum component, which dominates when the scene is "dim", i.e., at very high LOSTA. The lower part of Fig. 2 (part a) shows how the three noise components vary, at 12 μm wavelength in channel 5, with increasing "band photon radiance" (BPR). BPR is the photon radiance collected over the channel's entire spectral range, (after accounting for optics net spectral transmission and detector quantum efficiency), and determines the amplitude of the central fringes in the recorded interferogram. Photon noise increases as the square root of BPR, while A/D noise increases

directly with each factor-of-two reduction in gain. The three noise spectral radiances curves shown in part (a) are equal to one-tenth of the actual computed spectra so that they can be clearly distinguished from the curves in part (b).

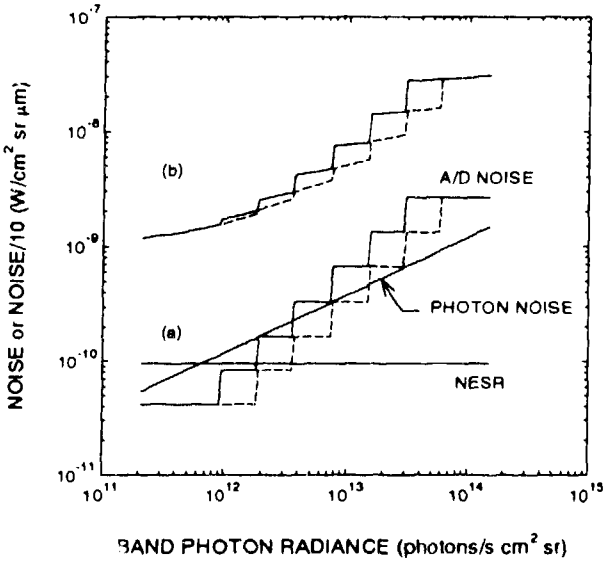

Figure 2. (a) The three components of total noise (times 0.1) versus "band photon radiance" for channel 5 at λ= 12 μm and for 1 cm^{-1} resolution. (b) The resultant total spectrum noise at λ = 12 μm.

In automatic mode the gain is increased (or decreased) when the interferogram's maximum value falls below (or rises above) certain threshold values. The new gain setting applies to the next interferogram. Different thresholds for gain increase and decrease provide the hysteresis needed for stability. Thus, the A/D noise can have one of two levels over a wide range of BPR, as indicated in Fig. 2, part (a). When the BPR continues to increase while the gain is at its lowest value, the interferogram's central fringes are eventually clipped; this occurs at the bottom end of the LOSTA ranges given in Table 1. Part (b) of Fig. 2 shows the typical behavior of spectrum total noise, equal to the root-sum-square of the three components.

Figure 3 shows preliminary, measured NESRs for the six interferometer channels for the highest resolution mode. The NESRs are lower for the other two resolution modes (and are reduced when the interferogram is apodized). The dashed portions of the curves for channels 3, 4 and 6 are extrapolated from the data; the "hump" in the NESR for channel 6 results from the prewhitening notch. The other two noise components (A/D and photon noise), being dependent on the observed scene, must be estimated case-by-case. A model of the interferometer system was developed, as a computer code, to obtain the spectrum of total noise given the NESR and a prediction of the scene spectral radiance. Since total noise and NESR have the same spectral shape, the computation amounts to a scaling operation. The code calculates the auto-gain level and resultant A/D noise contribution, and determines whether the interferogram will be clipped. It also produces a version of the given scene spectrum that has the IFR instrument line shape corresponding to a specified interferogram length and apodization function. It can be used to obtain a prediction of the NESR, based on data describing the system's optical components and electronics. An example of total spectrum noise is given in the following section.

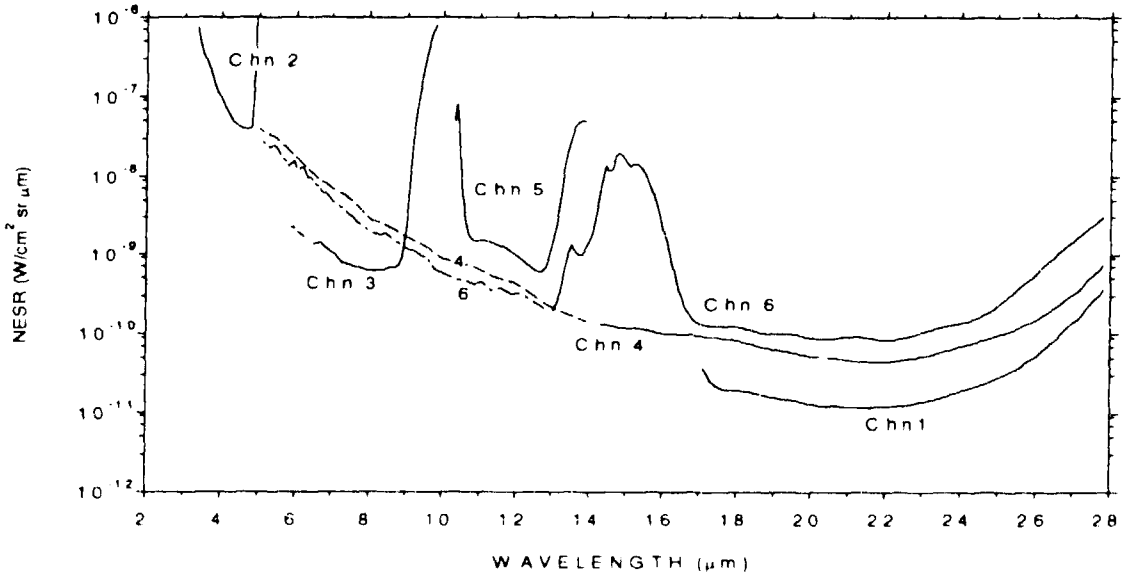

Figure 3. Preliminary measurements of the interferometer's six NESRs for the highest resolution mode, unapodized (1 cm^{-1} resolution in wavenumber).

4. PLANNED EXPERIMENTS

The planned MSX Earth Limb Experiments ELE-19 and ELE-10, entitled "Stratospheric Trace Gas Survey" and "Vertical Profile Survey," respectively, are designed to use the SPIRIT III interferometer (and the UVISI imaging spectrographs) to develop a "climatology" of earthlimb spectral radiance, to validate physical models of earthlimb radiance, and to recover vertical profiles of radiatively active species. Both experiments will scan the limb repetitively in a sawtooth fashion by moving the IFR's optic axis slowly from the lowest to highest tangent height and resetting rapidly back to the starting height; primary data is obtained only in the upward scan. Scanning the limb upward rather than downward implies lower gain, i.e., higher A/D noise, but avoids a significant loss of data (repeated clipping of the interferogram's central fringes prior to an automatic gain reduction in the downward scan). The upward scan rate will be on the order of one km/s. The resulting 4.3-km change in LOSTA as each long interferogram is recorded is found through simulations to produce minimal degradation of dominant emission features in the spectrum. ELE-19 will cover tangent altitudes from 6 to 70 km and use primarily data from IFR channels 5, 2 and 3. ELE-10 will scan over the 30-150 km range and use all channels of the IFR. Each data collection event (DCE) will consist of a series of these sawtooth scans, providing data over a wide range of latitudes and seasons. The DCEs will be repeated to generate useful statistics on the variability of trace gas concentrations.

Interferometer data from all experiments that use the IFR as the primary sensor or in a support role will undergo regular, *automated* analysis at the Phillips Laboratory Data Analysis Center as the data is received.[4] The purpose is to reduce the interferograms to calibrated spectra, provide for timely assessment of experiment performance, catalog the data, and generate catalog indices that flag particular phenomenologies or "events" for later review in the so-called *interactive* analysis. The events to be indexed, which have easily recognized effects in the spectrum, include auroral activity and stratospheric ozone depletion. Associated with each are a defined set of calculations that result in one or more "indicator" values, such as the factor by which a particular integrated band radiance exceeds a predicted quiescent value due to possible auroral enhancement during a period of high K_p. The indicator values, corresponding thresholds, and uncertainties in the indicator values computed from the noise model described earlier, are used to gauge the significance of the event and assign an index value to it. Generally, any large differences between measured and expected limb radiance spectra, where the latter are defined by a precomputed "template" library, will be flagged by a high index value. The templates for the IFR are maintained as interferograms so that they can be processed into spectra (as needed, during the automated processing) in the same manner as the data interferograms.

Retrieval of species vertical profiles from the reduced spectra imposes a much greater demand on computer resources than these data reduction and cataloging procedures, and will be part of the subsequent interactive analysis. Some interactive analyses of IFR spectra will use inferences drawn from supporting data provided by the UVISI system and from corollary measurements obtained by cooperating ground sites (e.g., ARM) and operational weather satellites (e.g., NOAA 11 and 12).

Figures 4 and 5 show typical computer-display color images (reproduced here in grey-scale) that will be produced as graphical display products for ELE-19; the displays for ELE-10 and other earthlimb experiments are similar. Information conveyed in these figures will be contained in files created in the automated processing, but is not displayed as a screen image until an investigator requests the display in the interactive review process. Figure 4 shows the measured spectra (actually template spectra in this illustration) when the IFR's optic axis is at 76.8 km. Each of the six figure panels, according to an option selected by the interactive user, includes the estimated total noise spectrum and shows the measured limb spectral radiance only where it exceeds the total noise. Figures 4 and 5 represent concepts; codes to produce them do not yet exist.

The top-central portion of the display in Fig. 4 gives basic date, time and pointing information, and shows options selected in the principal investigator's experiment script, such as the apodization function, which affects the spectral resolution and levels of sidelobes and noise in the displayed spectra. The IFOV map at the upper left is coded in six colors to correspond to the six displayed spectra. One can mouse-click on "buttons" in the upper right to view a new display showing the spectrum for only one channel on an expanded scale, and to superimpose the appropriate zodiacal background (ZOD) spectrum, an estimate of Non-Rejected Earth Spectral Radiance (NRESR) or the template spectrum; the latter three are generated routinely in the automated processing as each data interferogram is transformed to a spectrum. Figure 5 shows the result of a user's decision to display only the channel-3 spectrum, with ZOD, NRESR and template spectra superimposed. The upper panel indicates the location of the displayed spectrum and others measured in the ELE-19 sawtooth limb scan. Other interactive options in the two displays allow stepping over sequential spectrum sets within the current DCE or advancing to the next DCE.

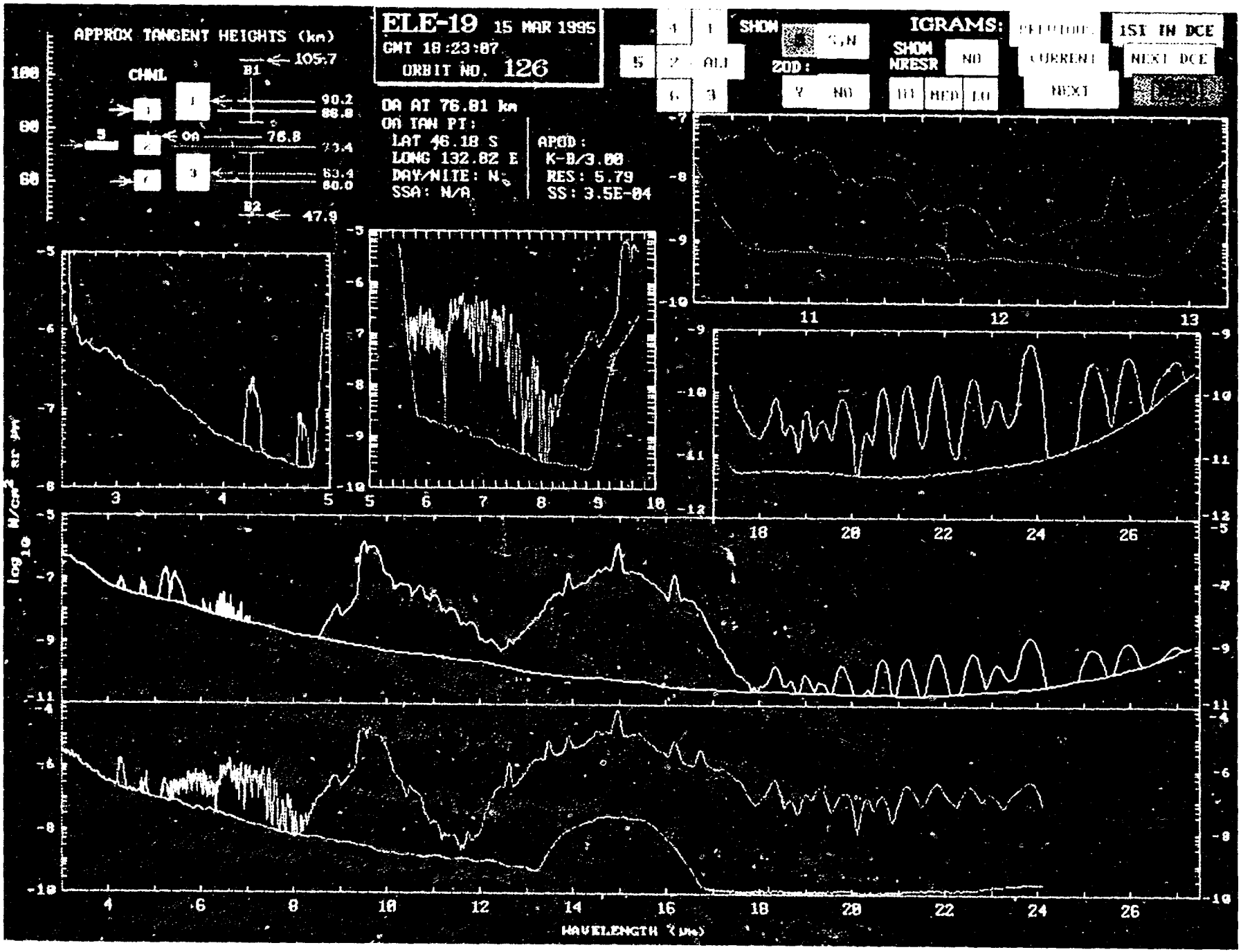

Figure 4—Simulated graphical display of ELE-19 data, all channels, processed to facilitate review and evaluation.

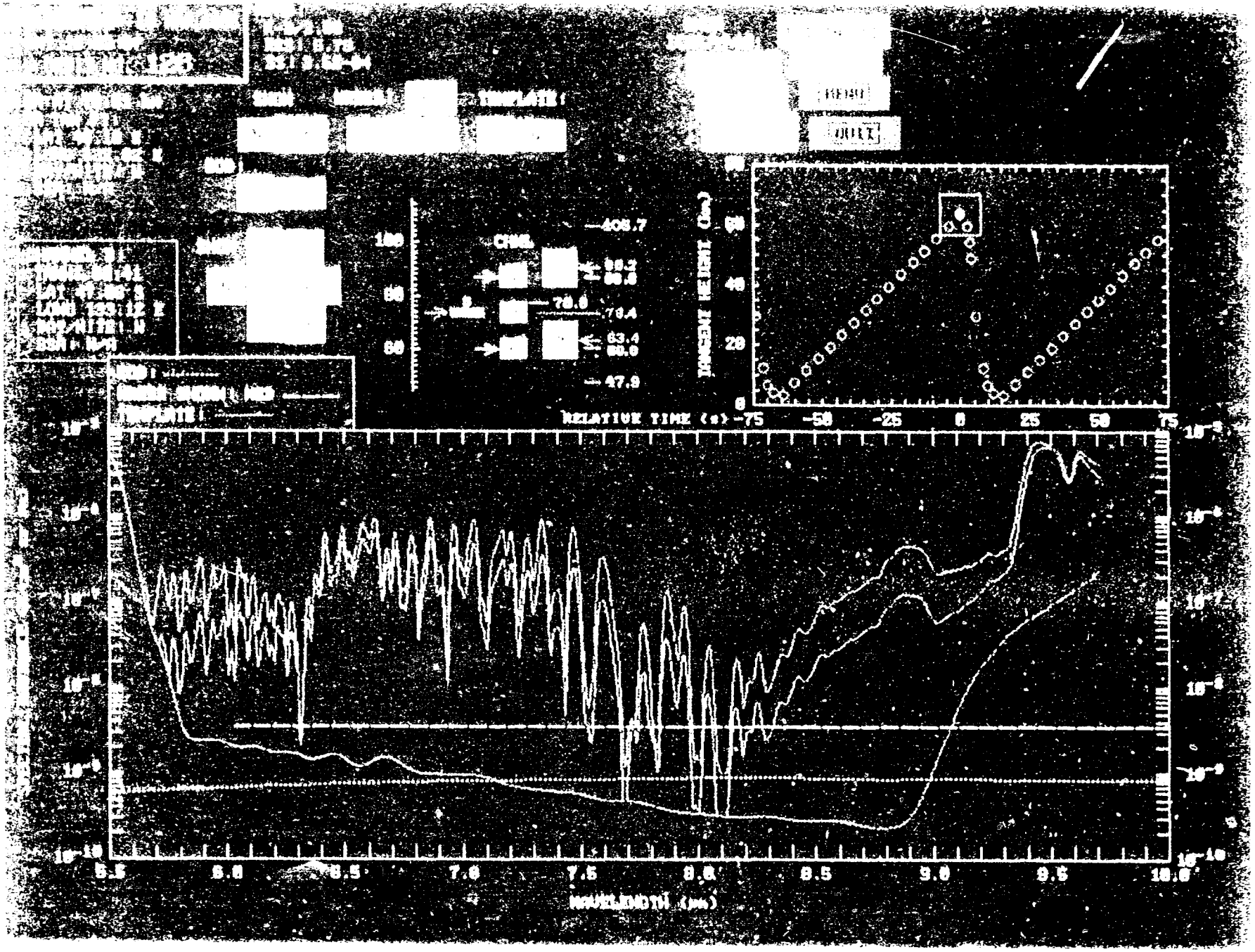
406.7
78.0
78.4
63.4
47.9
RELATIVE TIME (s) -75 -50 -25 0 25 50 75
WAVELENGTH (μm)
5.5 6.0 6.5 7.0 7.5 8.0 8.5 9.0 9.5 10.0

5. PREDICTED SENSING CAPABILITIES

Detailed computer simulations will be performed to quantify the expected precision and accuracy in species vertical profiles to be recovered from ELE-19 and ELE-10 data. Until these are completed, our estimates of remote sensing capability are based on calculations of "species contributions". In this context a contribution is defined as the effect a particular species has in the observed spectrum when introduced to an atmosphere that contains all but this species. By intercomparing the relative contributions of all expected species and total noise, for all IFR channels over a range of LOSTAs, one can at least estimate vertical ranges for the recovered profiles, if not accuracies in the species concentrations. This procedure, admittedly, is not as reliable or informative as the planned full-blown simulation and error analysis in which retrieval algorithms, like those described by Marks and Rodgers[11], will be applied to noise-contaminated synthetic data.

Figure 6 shows the total spectral radiance, predicted total system noise level and all significant species contributions over the wavelength range of channel 5 when its detector is centered on LOSTA = 15 km. The noise level is based on early estimates of performance and is expected to be somewhat lower when recalculated from final test data. The spectral resolution, corresponding to triangular apodization, is a constant 2 cm^{-1} in wavenumber. Calculation of these species contributions and total radiance used a version of the MODTRAN Code[12] modified by the Phillips Laboratory to include CCl_2F_2 (CFC-12 or F-12), CCl_3F (CFC-11 or F-11) and CCl_4. It is seen that these compounds, as well as nitric acid, ozone and CO_2, have contributions at LOSTA =15 km that do not seriously mask each other and are well above both the aerosol thermal background and sensor total noise level. The procedure to be used for the limb retrievals will attempt to recover these species simultaneously, using all wavelengths in the data spectrum.

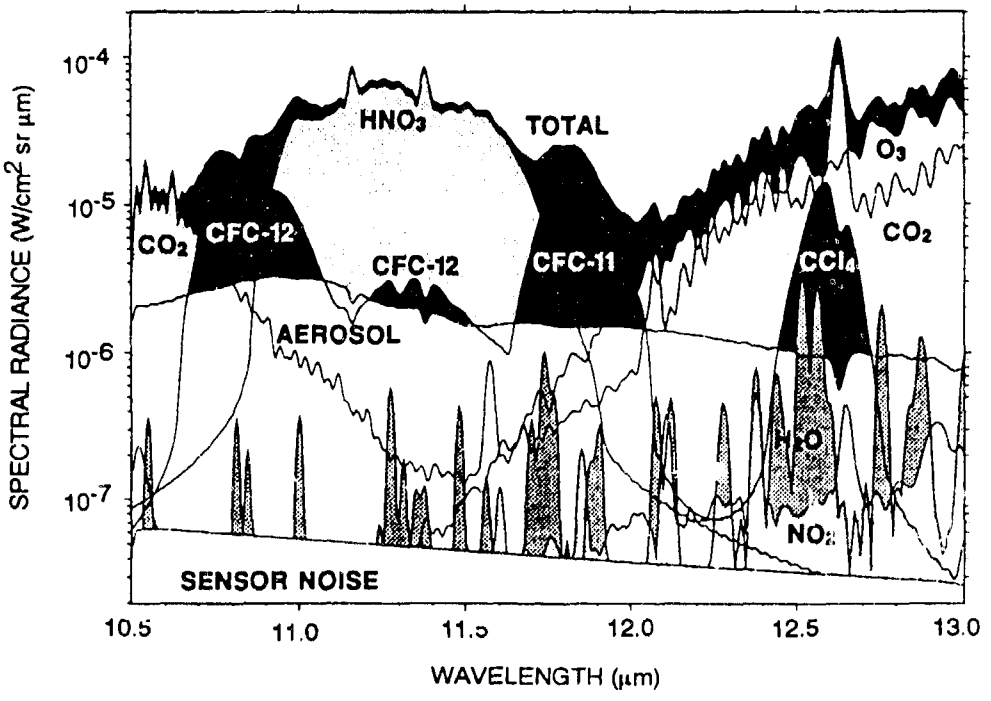

Figure 6. Species contributions and total noise computed for channel 5 for a tangent height of 15 km. The spectral signatures and interferometer noise level are early estimates corresponding to a spectral resolution of 2 cm^{-1}.

It was determined from similar calculations that the interferometer will be able to remotely sense the species/parameters appearing in Fig. 7, over the altitude ranges shown. Note that many of the species are detectable down to approximately 10 km, the LOSTA at which channel 5 is expected to be nearly saturated. The ultraviolet and visible instruments enhance the indicated IFR capability by adding some species and extending (during daytime) the ranges shown in Fig. 7 for NO_2 and aerosols.[13]

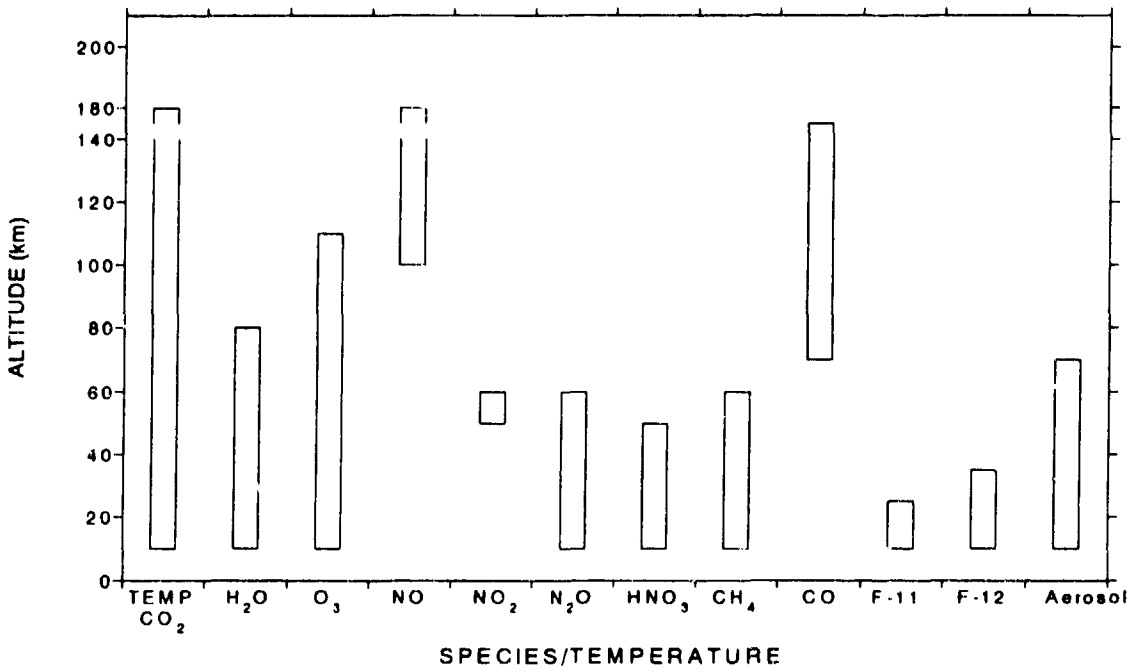

Figure 7. Measurement capabilities of the MSX SPIRIT III interferometer. The ordinate scale gives preliminary estimates of the tangent heights over which species vertical profiles can be retrieved.

6. SUMMARY

The comprehensive mission of the MSX program and its extensive instrumentation suits it well to the study of scientific issues having global significance, such as changes in the distributions of atmospheric trace species. The planned earthlimb observations include two interferometer experiments dedicated to measuring vertical profiles of NO, NO_2, N_2O, HNO_3, CH_4, CO, CFC-11, CFC-12, O_3, aerosols, H_2O and CO_2 over the altitude ranges shown in Fig. 7. These results will be supported by inferences drawn from MSX ultraviolet and visible measurements, and by data from corollary ground sites and weather satellites. The set of measured spectra, to be acquired over an 18-month period when no comparable data will be available from other satellite sensors, will give insight into chemical and dynamical processes affecting the global distributions of the above species, and provide evidence of short term changes in chemistry and climate.

7. ACKNOWLEDGMENT

The part of this research performed by the first author was sponsored by the Air Force Materiel Command under Contract No. F19628-93-C-0044.

8. REFERENCES

1. B. D. Guilmain, "Midcourse Space Experiment (MSX), an overview of the program, organization, targets, and schedule," Proc. SPIE 2232, page numbers to be assigned, 1994.

2. J. D. Mill, R. R. O'Neil, S. Price, G. J. Romick, O. M. Uy, E. M. Gasposchkin, G. C. Light, W. W. Moore, Jr., T. L. Murdock and A. T. Stair, "The Midcourse Space Experiment: An introduction to the spacecraft, instruments and scientific objectives," accepted for publication in the *Journal of Spacecraft and Rockets*.

3. J. D. Mill, "Midcourse Space Experiment (MSX), an overview of the instruments and data collection plans," Proc. SPIE 2232, page numbers to be assigned, 1994.

4. R. R. O'Neil, H. A. B. Gardiner, J. Gibson, C. H. Humphrey, R. Hegblom, M. E. Fraser, M. Kendra, P. Wintersteiner and C. Rice, "Midcourse Space Experiment (MSX): plans and capability for the measurement of infrared earthlimb and terrestrial backgrounds," Proc. SPIE 2223, page numbers to be assigned, 1994.

5. C. B. Farmer, O. F. Raper and F. G. O'Callaghan, "Final report on the first flight of the ATMOS instrument during the Spacelab 3 mission, April 29 through May 6, 1985," Jet Propulsion Laboratory Publication 87-32, October 1, 1987.

6. B. Bartschi, A. Steed, J. Blakeley, M. Ahmadjian, J. Griffin and R. Nadile, "Cryogenic infrared radiance instrumentation for shuttle (CIRRIS 1A) instrumentation and flight performance," Proc. SPIE 1765, pp. 64-74, July, 1992.

7. C. A. Reber, C. E. Trevathan, R. J. McNeal and M. R. Luther. "The Upper Atmosphere Research Satellite (UARS) mission," *J. Geophys. Res., 98,* pp. 10643-10647, June 20, 1993.

8. "EOS Reference Handbook," NASA Earth Science Report Office, Report No. NP-202, March 1993.

9. H. A. B. Gardiner, R. R. O'Neil, W. Grieder, R. Hegblom, C. H. Humphrey, W. Gallery, R. Sears and A. T. Stair, Jr., "Midcourse Space Experiment (MSX): planned observation of MWIR BTH and LATH Backgrounds," Proc. SPIE 2223, page numbers to be assigned, 1994.

10. "SPIRIT III Sensor User's Guide," Revision 3, Utah State University Space Dynamics Laboratory Report No. SDL/92-041, May 1993.

11. C. J. Marks and C. D. Rodgers, "A retrieval method for atmospheric composition from limb emission measurements," *J. Geophys. Res., 98,* pp. 14939-14953, August 1993.

12. A. Berk, L. S. Bernstein and D. C. Robertson, "MODTRAN: A moderate resolution model for LOWTRAN 7," Geophysics Laboratory, GL-TR-89-0122, April 1989, ADA214337.

13. G. J. Romick, D. E. Anderson, J. F. Carbary, L. J. Paxton, C. I. Meng and D. M. Morrison, "Midcourse Space Experiment satellite ultraviolet and visible background phenomenology," Proc. SPIE 2223, page numbers to be assigned, 1994.

REFERENCES

1. "SPIRIT III Sensor User's Guide," Revision 3, Utah State University Space Dynamics Laboratory Report No. SDL/92-041, May 1993.

2. A. S. Zachor, "Earthlimb Measurement Capabilities of the MSX SPIRIT III Interferometer Spectrometer," Final technical report on Subcontract No. 956-2, Atmospheric Radiation Consultants, Inc. Report No. ARC-TR-93-010, April 1993.

3. A. S. Zachor, "Noise Model of the MSX SPIRIT III Interferometer," Atmospheric Radiation Consultants, Inc. Report No. ARC-TR-93-011, July 1993.

4. "MSX: Earthlimb Automated Analysis Plan," Version 1.0, Physical Sciences Inc. Report No. PSI-1131/TR-1233, April 1993.

5. F. J. Harris, "On the Use of Windows for Harmonic Analysis with the Discrete Fourier Transform," *Proc. IEEE* **66**, 51 (1978).

6. C. Wyatt, "CIRRIS-1A Interferometer: Radiometric Analysis," *Appl. Opt.* **28**, 5069 (1989).

7. A. Berk, L. S. Bernstein and D. C. Robertson, "MODTRAN: A moderate resolution model for LOWTRAN 7," Geophysics Laboratory, GL-TR-89-0122, April 1989, ADA214337.

8. R. D. Sharma, A. J. Ratkowski, R. L. Sundberg, J. W. Duff, L. S. Bernstein, P. K. Acharya, J. H. Gruninger, D. C. Robertson and R. J. Healey, "Description of SHARC, The Strategic High-Altitude Radiance Code", Geophysics Laboratory, GL-TR-89-0229, 1989, ADA213806.